Contrib Mineral Petrol (2008) 155:329–340
DOI 10.1007/s00410-007-0245-1

ORIGINAL PAPER

Plagioclase in the Skaergaard intrusion. Part 1: Core and rim compositions in the layered series

Michael J. Toplis · William L. Brown · Elsa Pupier

Received: 12 April 2007 / Accepted: 7 August 2007 / Published online: 9 September 2007

Abstract The anorthite content of plagioclase grains (X_{An}) in 12 rocks from the layered series of the Skaergaard intrusion has been studied by electron microprobe (typically ~30 core and ~70 rim analyses per thin section). Mean core compositions vary continuously from An_{66} at the base of the layered series (LZa) to $An_{32–30}$ at the top. On the other hand, crystal rims are of approximately constant composition ($An_{50 \pm 1}$) from the LZa to the lower Middle Zone (MZ). Above the MZ, core and rim compositions generally overlap. Profiles across individual plagioclase grains from the lower zone show that most crystals have an external zone buffered at X_{An} ~50 ± 1. The simplest explanation for these features is that during postcumulus crystallization in the lower zone, interstitial liquids passed through a density maximum. This interpretation is consistent with proposed liquid lines of descent that predict silica enrichment of the liquid associated with the appearance of cumulus magnetite.

Communicated by T.L. Grove.

M. J. Toplis (✉)
UMR 5562 Dynamique Terrestre et Planétaire,
Observatoire Midi-Pyrénées,
14 avenue Edouard Belin, 31400 Toulouse, France
e-mail: toplis@dtp.obs-mip.fr

W. L. Brown · E. Pupier
UPR 2300 CRPG-CNRS,
BP 20, 54501 Vandoeuvre-Lès-Nancy, France
e-mail: billbr@crpg.cnrs-nancy.fr

E. Pupier
e-mail: elsa.pupier@free.fr

Keywords Skaergaard intrusion · Magmatic processes · Compositional convection · Plagioclase zoning

Introduction

The Skaergaard intrusion, East Greenland, is widely considered a case study for basaltic plutonism. Indeed, over the years, study of the Skaergaard has had a profound influence on our understanding of the physical and chemical processes taking place in mafic magma chambers (e.g., Wager and Deer 1939; Wager 1960, 1963; Wager et al. 1960; Wager and Brown 1968; McBirney and Noyes 1979; Irvine et al. 1998). However, despite intense study some fundamental aspects of the petrogenesis of the Skaergaard rocks continue to be the source of controversy, in particular the link between rock texture and magmatic processes (McBirney and Hunter 1995; Grant and Chalokwu 1998; Morse 1998), and the compositional evolution of the liquid during crystallization (Hunter and Sparks 1987, 1990; McBirney and Naslund 1990; Brooks and Nielsen 1990; Morse 1990; Tegner 1997). These controversies, concerning one of the most studied mafic layered intrusions in the world, highlight the fact that much remains to be learned about the workings of medium- to large-sized magma chambers in general. The question of the evolution of liquid composition is particularly important as the physical properties of the liquid phase (density, viscosity) will have a direct influence on the direction and rate of relative movements of solids and liquids during crystallization. On the other hand this reasoning implies that the modal proportions, textures, and geochemical characteristics of the rocks as we see them today may potentially provide insights into the physical and chemical evolution of the liquid during differentiation. With this idea in mind we have initiated a

detailed re-examination of the rocks from the Skaergaard with the aim of constraining the relative movements of crystals and liquids during solidification, and by inference the liquid line of descent, of this classic magma chamber.

The focus of our attention in this paper is the fate of interstitial liquids throughout the intrusion. This is because in a partially crystalline material consisting of accumulated crystals and an interstitial liquid, the texture and geochemistry of the final rock will critically depend on how the interstitial liquid is eliminated during cooling. This liquid could be consumed by in-situ crystallization in a closed system, expulsed by compaction, or buffered by some form of diffusional/convectional exchange, each of these possibilities having different implications for the evolution of the liquid.

Of all the potential markers of magmatic differentiation, we have chosen to study the major-element chemistry of plagioclase. Plagioclase is a particularly suitable marker of crystallization over a wide range of length scales because: (1) it is a ubiquitous phase throughout the Skaergaard (Wager and Brown 1968; Maaløe 1976; Naslund 1984; Hoover 1989; McBirney 1989; Jang and Naslund 2001) (2) its main compositional variation involves coupled chemical substitution of (Na, K) Si for CaAl, the interdiffusion of which is so slow that the original compositional profiles may be preserved on a scale of $<\sim 5$ μm, considerably smaller than the typical size of individual plagioclase grains (Morse 1984; Smith and Brown 1988, Fig. 17.25); (3) it is the only major mineral, besides olivine, which shows no microscopic exsolution; (4) its triclinic symmetry has the consequence that zoning can be well seen optically, so that suitable areas for detailed study are easily selected from standard thin sections.

Previous studies of plagioclase in the Skaergaard intrusion have shown the existence of generally homogeneous crystal cores thought to have crystallized early from a large volume of liquid, overgrown by often zoned postcumulus rims, interpreted to have crystallized in situ from a restricted volume of intercumulus liquid (e.g., Wager et al. 1960; Maaløe 1976). To extend these previous studies and to constrain the cumulus and early postcumulus processes in the Skaergaard intrusion, we have characterised in detail rim compositions of plagioclase throughout the $\sim 2{,}500$ m of the layered series (LS), and measured zoning profiles in individual plagioclase grains from the lower zone. Based upon these results we quantify the extent of the local liquid line of descent as a function of stratigraphic height, and discuss the implications of these results for the behaviour and properties of the intercumulus liquid. Detailed consideration of the most extreme overgrowths and their spatial distribution throughout the Skaergaard magma chamber will be the object of a companion paper (W.L. Brown and M.J. Toplis, in preparation).

The Skaergaard intrusion

The Skaergaard intrusion has been described many times in the literature and a summary of only the most salient features is presented here. For a more detailed description the reader is referred to Wager and Brown (1968) and McBirney (1996a). The intrusion (Fig. 1) is roughly oval in shape (~ 11 by ~ 8 km and ~ 4–5 km thick), and thought to be fault-bounded (Irvine et al. 1998; Nielsen 2004). It is divided structurally into a generally steep marginal border series (MBS) which crystallized inwards from the walls, inside of which are found a gently dipping LS which crystallized upwards from the unexposed floor and a gently dipping upper border series (UBS) which crystallized downwards from the roof, now mainly eroded. Rocks in the LS generally show well-developed layering and igneous

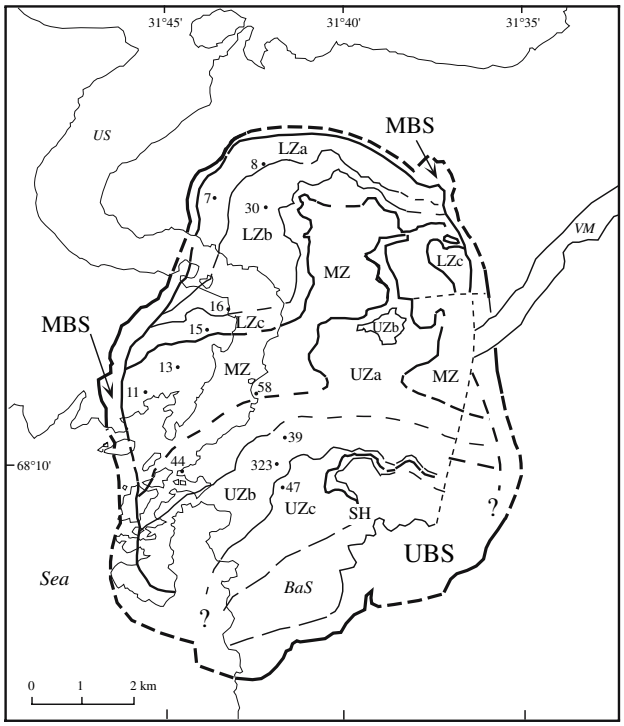

Fig. 1 Simplified geological map of the Skaergaard intrusion (modified after Irvine et al. 1998) showing the Marginal Border Series (*MBS*), the Upper Border Series (*UBS*), and the different subzones of the layered series (*Lza–c*, *MZ* and *Uza–c*). The Uttental Sound (*US*) and sea are indicated as convenient references. The inferred position of the Sandwich Horizon (*SH*) is shown by a *thick line* between UZc and the equivalent rocks in the UBS to the W and N of Basistoppen. Rocks closest to the southern contact are shown belonging to the UBS although there is evidence of a discontinuity which would suggest that they should be included in the MBS (cf. Naslund 1984 and the geological map of McBirney 1996a, b). The later Basistoppen Sheet (*BaS*) in the S and Vandfaldsdalen Macrodyke (*VM*) in the NE are also shown. Geological relationships in the S and SE are obscure, as shown by a *question mark*. The positions of the specimens studied are shown by a *dot* and a *number*

lamination which dip gently to the SSE at 15°–25° (Wager and Deer 1939; Wager and Brown 1968; McBirney 1996b; Nielsen 2004), so that over 3.5 km thickness of layered rocks is seen.

Each Series shows a succession of cumulus minerals which appear in the same order and show similar cryptic variation from the outside to the centre of the intrusion (Wager 1960; Wager and Brown 1968; Maaløe 1976; Naslund 1984; Hoover 1989; McBirney 1989, 1996a; Irvine et al. 1998; Jang and Naslund 2001). These observations have been taken as evidence that the cumulus part in all three Series arose by fractional crystallization of a single pulse of magma, essentially along a single liquid line of descent (LLD), although there is some isotopic evidence for a second input of magma in the lower zone (Stewart and DePaolo 1990). All three Series have been divided into a number of similar (sub)zones. The LS was divided into a lower zone (LZ), a middle zone (MZ) and an upper zone (UZ) on the basis of the presence of cumulus olivine in the LZ and UZ and its absence in the MZ (Wager 1960); the MBS and UBS were similarly divided, but use was also made of the composition of the plagioclase (Wager 1960; Wager and Brown 1968; Naslund 1984; Hoover 1989). The main zones in the LS were further subdivided into subzones (Wager 1960) on the basis of the absence of cumulus augite (LZa), the successive appearances of cumulus augite (LZb), magnetite (LZc), apatite (UZb) and ferrobustamite inverted to hedenbergite (UZc). Some of these zone boundaries are extremely sharp and visible in the field, such as the sudden appearance of layers with cumulus magnetite at the base of LZc or cumulus apatite at that of UZb.

In terms of petrology, plagioclase is by far the most wide-spread and abundant cumulus mineral in rocks of the Skaergaard intrusion (Wager and Brown 1968; Maaløe 1976; Naslund 1984; Hoover 1989; McBirney 1989, 1996a; Tegner 1997; Irvine et al. 1998; Jang and Naslund 2001), and was the first mineral to crystallize, along with olivine where present, in almost all rocks (Maaløe 1976). The average layered rocks in the lower zone of the LS are leucocratic olivine gabbros (frequently olivine pigeonite gabbros or gabbronorites), but more extreme leuco or mela varieties are not uncommon. Rocks in the MZ are olivine-free and change from pigeonite gabbro(norite) to pigeonite augite (mela)diorite, whereas the rocks in the UZ are (quartz) olivine ferroaugite (mela)diorites. Pigeonite as such no longer exists in rocks from the LZa to UZa of the LS, but has inverted to orthopyroxene with exsolved augite (Wager and Brown 1968). The gabbro(norite)s of the LZa,b are (poikilitic) orthocumulates, whereas the (gabbro)diorites of LZc, MZ and UZ are ad- to meso-cumulates (Wager et al. 1960; Wager and Brown 1968; Morse 1998).

Choice of specimens and methods of study

Thin sections of ~65 rocks from the LS were first examined optically to select those for more detailed study, in which the plagioclase was especially fresh, transparent and suitable for electron microprobe analysis. Most thin sections were orientated perpendicular to the layering and the igneous lamination. The latter is defined by the {010} faces of the plagioclase crystals, so that most of the plagioclase–plagioclase contacts are along (010) or close to it. On the basis of this preliminary study 12 polished thin sections were selected for detailed study, covering all sub-zones of the layered series (outcrops as shown on Fig. 1). All of the selected samples are typical *unlayered* rocks, exotic samples such as rare replacive rocks (McBirney and Sonnenthal 1990; McBirney and Hunter 1995; Irvine et al. 1998) not being considered suitable. The stratigraphic heights of the specimens studied were calculated from their position relative to the subzone boundaries and the layering using the stratigraphic section of Wager and Brown (1968) as a reference. The relative positions in the section are probably precise to ±25 m, but the absolute uncertainty in reported height may be up to 100 m, given the spread in reported thickness of individual sub-zones (e.g., Nielsen 2004). The selected thin sections were examined optically and by Scanning Electron Microscopy (SEM) to select the best areas for electron microprobe analysis. Electron microprobe analyses were made using a Cameca SX50 operating under normal working conditions of 15 kV and 10 nA. Natural mineral standards were used for calibration and counting times were typically 10 s. Errors in the calculated An contents of plagioclase expressed as mol% are approximately 1–2 mol%.

Results

Optical microscopy

Inter- and intra-crystalline textures of plagioclase

Plagioclase occurs usually as fairly large crystals, typically several millimetres in length, which decrease in modal proportion from the LZ towards the UZ. The crystals are tabular, subhedral on {010}, and generally define a well-developed igneous lamination. Multiple plagioclase/plagioclase contacts (self-contacts) are common in the LZ in which plagioclase is the most abundant mineral, whereas in the UZ plagioclase tends to form an open touching framework in which triple and higher contacts are rarer. Plagioclase contacts show no sign of textural equilibration (cf. Hunter 1996, Fig. 9D), so that we infer that the compositions measured near plagioclase rims have suffered little

modification; this is further supported by the observation that disequilibrium occurs on a small scale in the normal layered rocks of the LS, as illustrated by the fact that quartz frequently occurs in small pockets of low-temperature overgrowths less than 1 mm from moderately Mg-rich olivine (Wager and Brown 1968; W.L. Brown and M.J. Toplis, in preparation). In some rocks from the LZa plagioclase of two distinct sizes occurs, the larger crystals being tabular and discrete, whereas the smaller ones may touch each other at quite high angles to (010) and may occasionally interpenetrate. Where poikilitic augite is abundant it may enclose small partly discrete plagioclase crystals; most such rocks contain too much augite to be pure orthocumulates and a large proportion of it may have a heteradcumulate-like origin (Morse 1998; see also McBirney and Hunter 1995, Fig. 2; Henderson 1970). Nielsen (2004, p. 523) stated that "the last formed gabbros [melatdiorites in reality] in the LS (UZc) are often interpreted as cumulates, but their texture is often more like granulite-facies rocks, showing corona textures and significant amounts of trapped granophyric melt". We examined five rocks from the UZc and could see no evidence of corona textures nor of re-equilibration, plagioclase/plagioclase grain boundaries being often sutured and the inverted ferrobustamite showing a highly complex irregular polycrystalline texture (cf. Wager and Brown 1968, Fig. 20b). On the other hand thin coronas of olivine between Fe–Ti oxides and augite are frequent in LZc and MZ rocks (cf. Wager and Brown 1968, Figs. 41, 42) and the grain boundaries of augite and inverted pigeonite have adjusted on a microscopic scale to the exsolution microtexture.

In terms of evidence for plastic deformation under the optical microscope, we note that glide twins in plagioclase are common in LZc to UZa, less frequent in LZb and UZb and rare in LZa and UZc. Bent crystals are less frequent and have a more restricted range from LZb to UZb, being most common in LZc to UZa. Crystals with misorientated subgrains are not frequent, even in the MZ, and are seen only where the crystals are particularly long and thin, often occurring at prominent contacts with large ferromagnesian minerals. Weakly plastically deformed plagioclase thus occurs in typical (poikilitic) orthocumulates from the LZ through nearly perfect adcumulates of the MZ to imperfect ad- to mesocumulates of the UZ.

Cumulus and postcumulus zoning patterns

Our own observations under the optical microscope, complemented by those described in the literature, show that the plagioclase crystals consist of a central core of nearly homogeneous composition and a rim, which may show weak to strong normal zoning to more Ab-rich compositions (Wager and Brown 1968), although reverse zoning may be present inside the normal rims in plagioclases from the LZa (Maaløe 1976). The cumulus cores have a nearly constant composition in a given layer and also in adjacent layers; for example, Jang and Naslund (2001) obtained a composition of $An_{48.77 \pm 1.35}$ for plagioclase separates from six adcumulate samples at a stratigraphic height of ~860 m in the lower MZ along a 6 km traverse from Kraemer Island to near Uttental Plateau and $An_{43.31 \pm 1.14}$ for three samples at ~1,500 m from the upper MZ. The cumulus cores are largely unzoned except at the very base of the intrusion (Maaløe 1976) and at the top of the roof zone (Naslund 1984). In these cases, complex cores occur, consisting of two optically distinct areas which may differ in An content by a few mol% (well seen in specimen PSK7 from near the lowest exposures of LZa). The cumulus cores form a significant volume proportion of the plagioclase crystals, in the range 50–95%, the proportion being lower in (poikilitic) orthocumulates of the LZa,b than in ad- and meso-cumulates of LZc, MZ and UZ (Wager et al. 1960; Wager 1963; Wager and Brown 1968; Henderson 1970; Paster et al. 1974; Maaløe 1976). Optically, the more Ab-rich rim varies greatly in thickness, and may in certain cases be absent (see below). The more Ab-rich rims are thickest in the (poikilitic) orthocumulates from the LZa and LZb (PSK7 and PSK8), but become progressively thinner and closer in composition to the core from LZa to LZb (PSK16); they are generally absent in LZc (PSK15), MZ and UZa, with some exceptions near the Triple Group at the top of the MZ where postcumulus olivine (Andersen et al. 1998) and quartz (Wager and Brown 1968) may occasionally occur.

Electron microprobe analyses

Core compositions

For each thin section an average of ~30 plagioclase cores have been analysed. Histograms of the distribution of core compositions for each sample show that anorthite content shows a broadly symmetric distribution around a well defined maximum in the mode (Fig. 2). In general 50% of the compositions lie within ±1(to 2) mol% and 90% within ±2 to 3 mol% of the mean (Table 1). This degree of variability is barely greater than the analytical errors associated with each individual analysis (1–2 mol%) and is of a comparable magnitude to that reported by Tegner (1997) for 38 samples from the top of the MZ to UZc. The one exception is sample PSK7 (the stratigraphically lowest rock considered here) in which plagioclase cores have a wider distribution of composition (Fig. 2; Table 1). However, as noted above, this specimen shows optically complex cores with areas of two different compositions

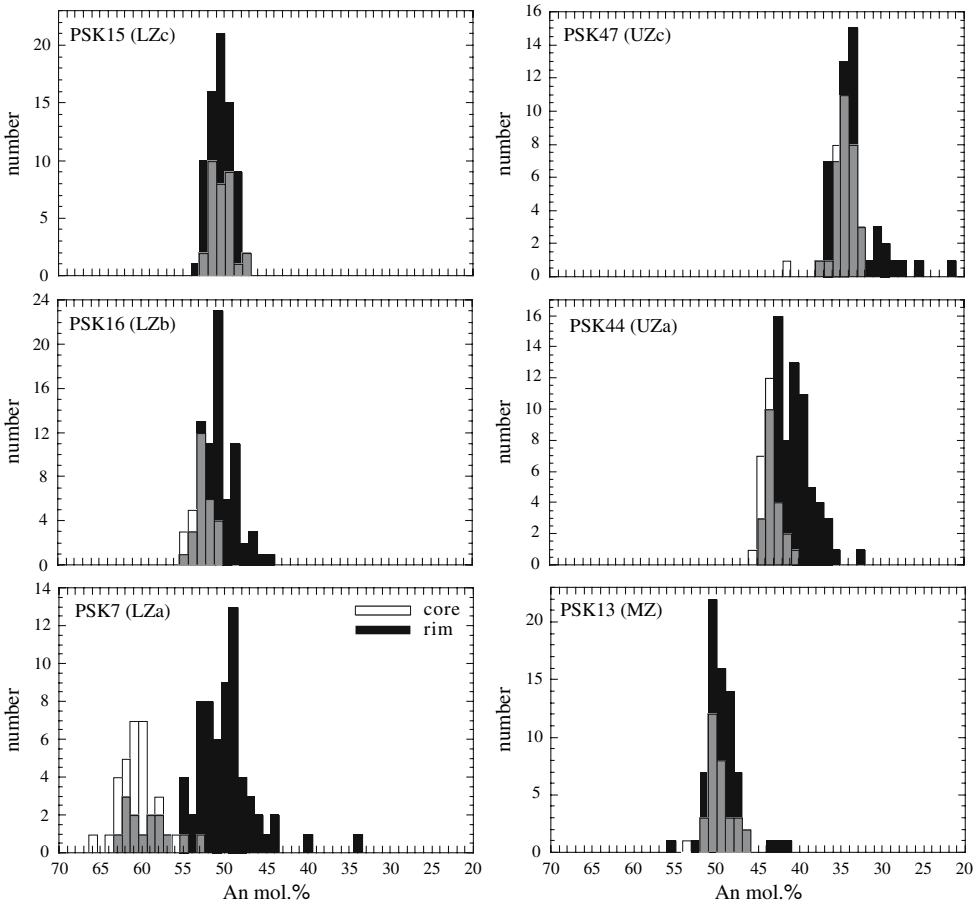

Fig. 2 Histograms for six specimens from the LS as a function of mol% An; cumulus core compositions are shown in *white*, plagioclase/plagioclase rim contact compositions in *black*, and where they overlap, in *grey*

which were not separately studied, the probe spots having been selected using the back-scattered electron imaging mode of the electron microprobe under which conditions, small compositional differences are not easily visible. We also note that Parsons and Lee (personal communication) made 20–40 microprobe analyses per sample of plagioclase cores for the PSK specimens. Those results indicate a one standard deviation of $\pm An_{1.0-2.2}$, except for PSK7 and PSK8 for which the standard deviation was $\pm An_{3.6-4}$, in excellent agreement with the findings of this study.

When plagioclase core compositions are plotted as a function of stratigraphic height, a linear dependence of X_{An} on height may be fitted to the data if the whole range of observed core compositions in each rock is considered (Fig. 3). This first order fit to the data implies an average change of –1.2 X_{An} per 100 m of stratigraphy, or 80 m of stratigraphy per mol.% An. In other words an observed range in core compositions of ±2 mol% An corresponds to a fictive difference in stratigraphic height of almost ±200 m. However, in detail, if only the mean values of core composition are considered there is clear evidence that the variation of X_{An} with height is non-linear, variation being smaller across the MZ compared to the LZ and UZ (Fig. 3), corroborating a similar conclusion reached by Maaløe (1976).

Rim compositions

For each thin section an average of ~70 plagioclase rims have been analysed, measurements being made approximately 5 μm from the edge of the crystal. Histograms of these compositions show that in samples from LZb to MZ the range of X_{An} is narrower than in rocks from LZa, UZb and UZc (Fig. 2; Table 1). Indeed, the histograms of rims for specimens from the LZc and MZ are generally as narrow as, or narrower than, those of the cumulus cores. On the other hand, samples from the LZa, UZb and especially UZc have numerous outliers of significantly lower An content than the mean (Fig. 2; Table 1), found to be associated with pockets of lower-temperature granophyric material. Nevertheless, histograms of the compositions of plagioclase rims show a well-defined peak in the mode, in particular for rocks from the LZ and MZ (Fig. 2). Somewhat surprisingly, for almost all the specimens from the LZ, the composition of the mode (and to a lesser extent the

Table 1 Summary of the plagioclase compositions in each rock studied

Sample name	(Sub) Zone	Height (m)		*n*	90+	50+	Mean	50–	90–
PSK7	Lza	120	Cores	34	65.0	62.4	61.3	59.7	55.1
			All rims	77	62.3	53.9	51.1	49.3	45.0
			Self-contacts	45	61.7	51.1	49.7	48.6	44.3
PSK8	LZa/b	250	Cores	31	64.2	62.5	61.4	60.6	58.0
			All rims	77	63.5	56.0	54.2	52.9	50.9
			Self-contacts	22	54.2	51.6	50.9	49.9	45.4
BM30	LZb	460	Cores	31	58.6	57.5	57.1	56.8	52.4
			All rims	71	57.3	55.2	53.7	52.6	50.6
			Self-contacts	21	56.5	54.8	53.0	52.4	50.0
PSK16	LZb	650	Cores	31	54.9	53.5	52.6	52.0	50.9
			All rims	76	53.5	52.2	50.7	49.4	46.8
			Self-contacts	45	53.0	51.6	50.6	49.0	46.7
PSK15	LZc	750	Cores	32	53.0	51.8	50.9	49.9	48.0
			All rims	74	52.4	51.4	50.5	49.6	48.3
			Self-contacts	24	52.0	50.9	50.2	49.1	48.3
PSK13	MZ	900	Cores	32	52.2	50.8	50.2	49.1	46.8
			All rims	75	51.6	50.3	49.3	48.6	46.5
			Self-contacts	35	51.6	50.0	48.9	47.9	43.0
PSK11	MZ	1,150	Cores	26	51.2	50.7	49.4	47.4	44.2
			All rims	50	49.8	47.2	45.4	44.1	42.8
MZ58	MZ	1,500	Cores	29	49.1	48.1	47.0	44.4	42.5
			All rims	106	47.5	46.4	44.7	43.7	41.0
PSK44	UZa	1,650	Cores	27	44.9	44.1	43.4	42.8	41.4
			All rims	75	43.8	42.6	40.9	39.4	36.9
PSK39	UZb	1,900	Cores	31	41.1	39.6	38.6	37.9	37.2
			All rims	58	42.2	40.0	39.3	38.0	31.5
UB323	UZb	2,275	Cores	31	37.9	36.8	36.0	35.4	33.3
			All rims	54	37.3	36.5	35.4	33.8	23.4
PSK47	UZc	2,350	Cores	33	37.7	35.0	34.7	33.7	32.2
			All rims	58	36.7	35.1	34.0	33.0	27.6

About 90% of measurements centred on the mean occur between the bounds 90+ and 90–, while 50% of measurements occur between the bounds 50+ and 50–

corresponding mean; Table 1) has a constant composition of $An_{50 \pm 1}$ (see Fig. 2). Furthermore, if only the sub-set of analyses which concern plagioclase self-contacts (plagioclase in contact with another plagioclase) are considered, it is found that the constant nature of rim composition throughout the LZ is even more pronounced (Table 1; Fig. 4). For example, in PSK7 from the base of the LZ, plagioclase–plagioclase contacts have an extremely sharp peak in the mode at a composition $An_{49–50}$, while plagioclase rims in contact with other minerals (olivine and pyroxene) are on average richer in anorthite component, the most abundant rims having a composition $An_{53–54}$ (illustrated in Fig. 5). Another point of note is that the most evolved rims in contact with olivine or pyroxene reach compositions no lower than $An_{49–50}$ (Fig. 5). These differences are observed in the other rocks of LZa and LZb, and confirmed by compositional profiles across individual grains, as presented below. On the other hand, in and above the LZc, no significant difference between the mean composition of plagioclase self-contacts and that of the complete data set can be discerned (Table 1).

When the range and mean compositions of plagioclase self-contacts are plotted as a function of stratigraphic height (Fig. 4), a clear non-linearity is present, with a break in slope near the top of the LZc. This is even more apparent in a plot of mean core and rim compositions (Fig. 6) in which the convergence at $An_{50 \pm 1}$ at the top of the LZc can be clearly seen. Furthermore, this plot confirms and quantifies the petrographic observation that zoning is more extensive in the LZa and that the difference between core and rim compositions decreases with increasing stratigraphic height throughout the LZ. As an aside, we note that in the LZ, compositions of plagioclase separates determined by Jang and Naslund (2001) generally plot between our mean core and rim compositions, suggesting that those authors analysed something close to the bulk plagioclase

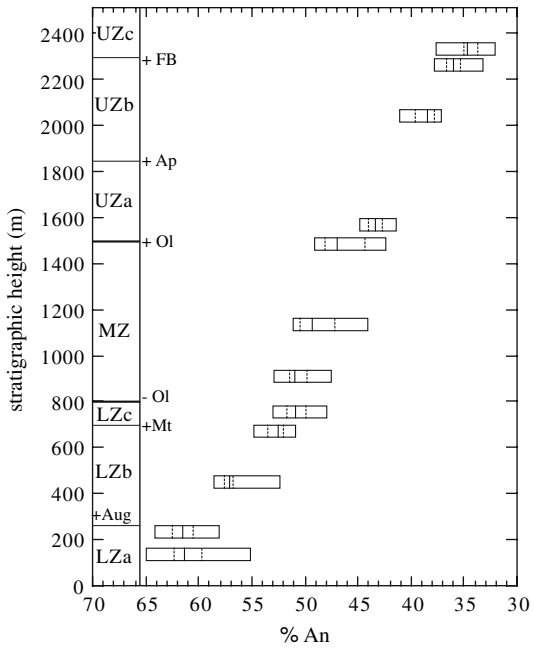

Fig. 3 Cumulus core compositions as a function of stratigraphic height. For each rock the mean is indicated by a *solid vertical line*. The *box* contains the 90% of the data closest to the mean and the two *dashed lines* represent the range of composition containing the 50% of the data closest to the mean

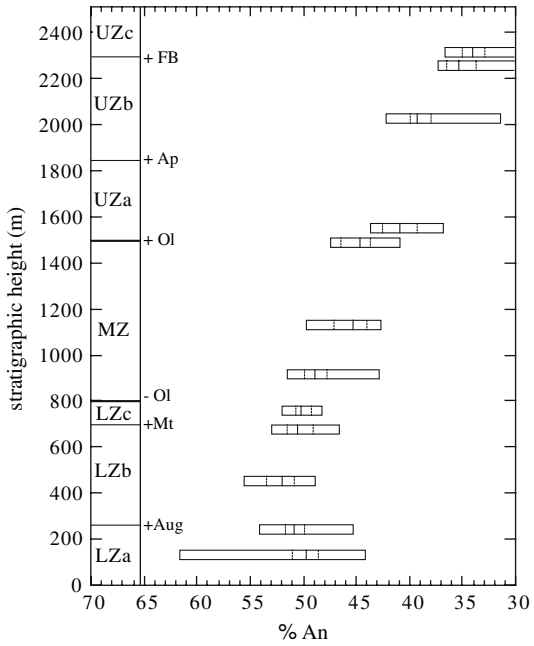

Fig. 4 Plagioclase self-contact compositions of as a function of stratigraphic height. For each rock the mean is indicated by a *solid vertical line*. The *box* contains the 90% of the data closest to the mean and the two *dashed lines* represent the range of composition containing the 50% of the data closest to the mean

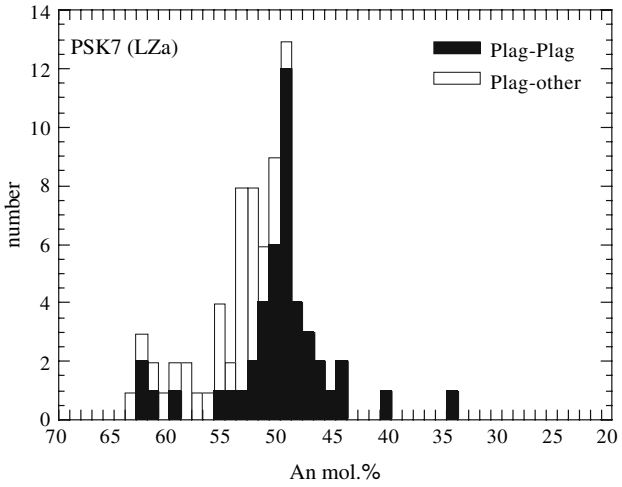

Fig. 5 Histogram of the compositions of plagioclase–plagioclase contacts (*filled bars*) and plagioclase-other contacts (*open bars*) for sample PSK7 from the LZa. Note that in this figure the data for different types of contact are stacked and not overlapped

composition. Analysis of bulk plagioclase composition by Jang and Naslund (2001) can also explain the excellent agreement between the two studies in the MZ and UZa (Fig. 6) where plagioclase crystals are not significantly zoned, and the observed offset to lower X_{An} in the UZb and UZc, resulting from the increasing abundance of evolved overgrowths (e.g., Fig. 2).

Zoning profiles in the lower zone

To complement the information provided by single measurements at crystal edges, we have also measured core-rim profiles in the zoned grains of the lower zone. For this purpose optical microscopy was used to select grains oriented perpendicular to {010}, which were then analysed by electron microprobe. Profiles were generally measured from one edge to another along a straight line. Between 20 and 50 points were analysed per profile, the distance between individual analyses varying from 8 to 100 μm.

Several types of zoning patterns are found as illustrated in Fig. 7. For certain grains, the central plateau of cumulus composition is in direct contact with the adjacent phase with no zoning of X_{An} (e.g., Fig. 7a). However, this situation is relatively rare and generally limited to plagioclase grains in contact with olivine (in LZa) or pyroxene (in LZb). Only one profile of a plagioclase in contact with an Fe–Ti oxide was made in the LZa and in this case the plagioclase is zoned, the X_{An} at the contact with the oxide being An_{50} (Fig. 7b). Compositional profiles towards plagioclase self-contacts are always zoned and typically reach

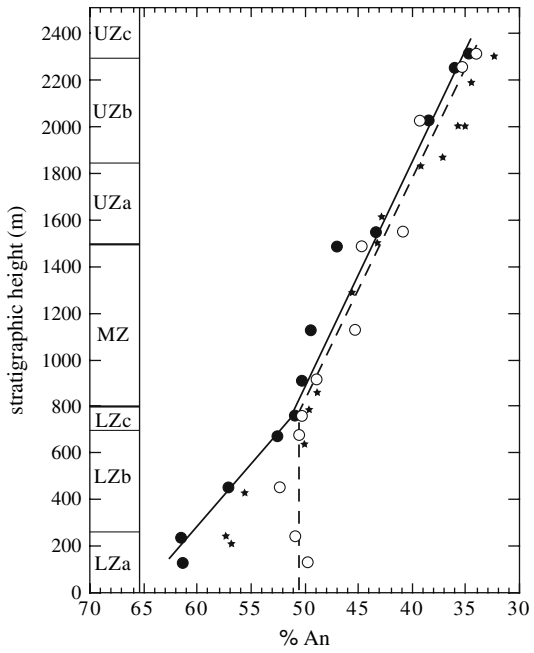

Fig. 6 Comparison of the mean core and rim compositions as a function of stratigraphic height. *Filled circles* are data for cores and *open circles* are data for self-contact rims. The *solid* and *dashed lines* are guides for the eyes and represent the variation of core and rim composition, respectively. *Stars* indicate the data of Jang and Naslund (2001), as discussed in more detail in the text

An_{50} at the rim (Fig. 7a–c), consistent with the results presented above. An identical finding was made by Shimizu (1978) who measured a single profile across a plagioclase grain from the LZb using the ion microprobe. However, we find that the majority of profiles towards a plagioclase–plagioclase contact consist of three discrete sections; a central zone of cumulus composition, a relatively narrow zone of decreasing X_{An} and an external zone, of variable width, over which X_{An} has a constant value (Figs. 7c, 8). Considering data for grains throughout the lower zone (Fig. 8) we can confirm that the X_{An} of core composition decreases with increasing stratigraphic height, and that the compositions of plagioclase self-contacts are approximately independent of stratigraphy. However, we highlight the fact that plagioclase crystals typically show an extensive external zone, of variable width, which is buffered at a composition of $An_{50 \pm 1}$ (Fig. 8), a feature which could not be inferred from the histograms of individual analyses at plagioclase grain edges.

Discussion

The variation of plagioclase core composition as a function of stratigraphic height has been described many times in the literature (e.g., Wager 1960) and from this point of view the data presented here provide no fundamental new insights into the cumulus trend, merely supporting the hypothesis of fractional crystallization of a single pulse of magma. On the other hand, the systematic and characteristic variations of rim compositions and zoning profiles, in particular in the lower zone, have received much less attention, and no petrogenetic model has been proposed to explain them. In the following discussion we will interpret these features in terms of local magmatic processes occurring during crystallization of the intercumulus liquid,

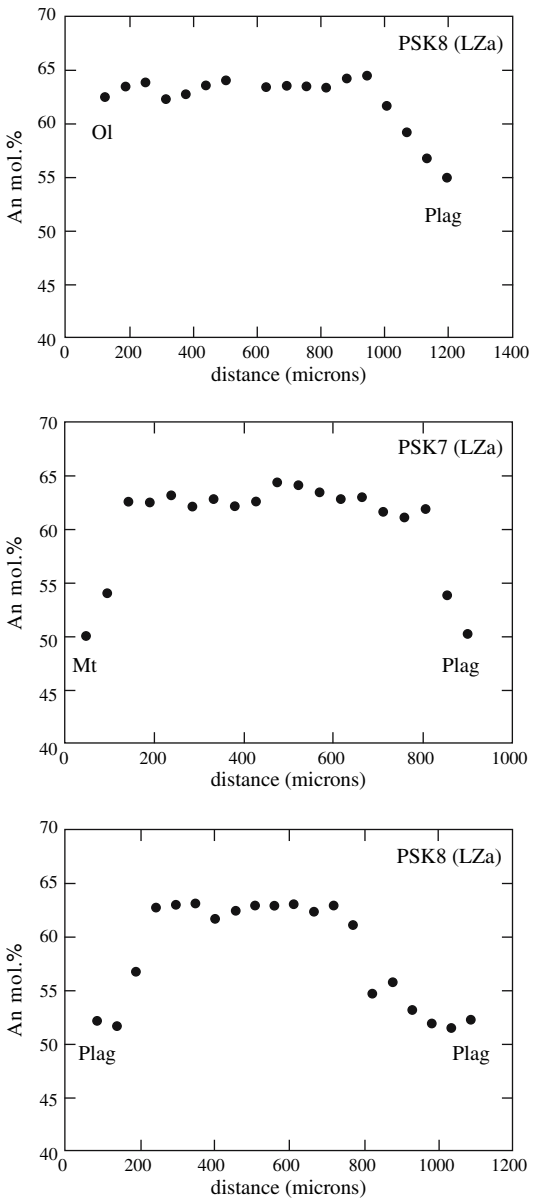

Fig. 7 Compositional profiles across representative plagioclase grains from samples from the lower zone a, as indicated. The nature of the phase in contact with the plagioclase is indicated. The distance scale is from an arbitrary starting point and only relative distances have any significance

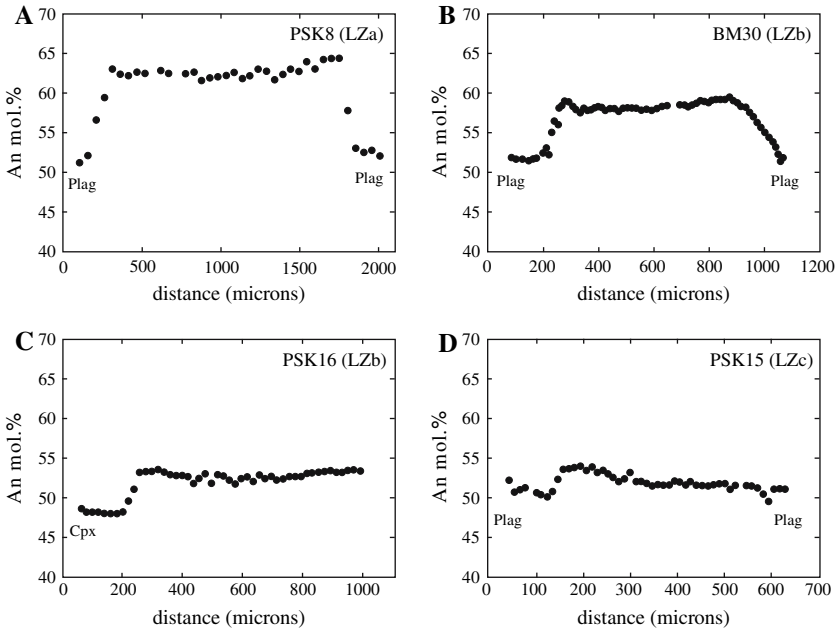

Fig. 8 Compositional profiles across representative plagioclase grains from throughout the lower zone, as indicated. The nature of the phase in contact with the plagioclase is indicated. The distance scale is from an arbitrary starting point and only relative distances have any significance

assuming that X_{An} is an unperturbed marker of local differentiation, as discussed above.

First of all, we note that if intercumulus liquids in the crystallizing front were always immobile, such that crystallization took place in situ without exchange of matter with overlying or underlying liquids, then overgrowths on cumulus plagioclase grains throughout the intrusion should systematically reach compositions approaching pure albite. This is because, in the absence of adcumulus growth mechanisms, the products of the *whole liquid line of descent* should be present *in all rocks*, a situation frequently encountered in small to medium-sized sills (e.g., Henderson and Gibb 1983; Gibb and Henderson 1996). This is clearly not true of any of the samples studied here, and particularly so for rocks of the MZ and UZa which show no compositionally distinct overgrowth zones whatsoever. In this case it is clear that some mechanism must have existed for expulsion of the intercumulus liquid from the framework (compaction), and/or for efficient convectional/diffusional exchange with the overlying main liquid. Furthermore, if one considers the zoning patterns in rocks of the lower zone, it would appear that mobility or elimination of the intercumulus liquid was preceded by a period of in-situ crystallization.

Based upon the rocks of the MZ and UZ alone it is difficult to distinguish between the different hypotheses for elimination of postcumulus liquid. In other large layered intrusions such as the Stillwater complex, compaction has been proposed as the dominant mechanism of liquid extraction (e.g., Meurer and Boudreau 1998; Meurer and Meurer 2006). However, we note that if compaction were the only mechanism of expulsion of gravitationally stable intercumulus liquids in the Skaergaard, it is difficult to rationalize why this process would have been most efficient at intermediate stratigraphic levels, given that compaction is qualitatively favoured by increasing thickness and weight of the overlying layers. Furthermore, in the lower zone, compaction alone is difficult to reconcile with the fact that the inferred onset of liquid mobility occurs at the same point along the liquid line of descent for rocks from different stratigraphic levels (Fig. 6). In addition, compaction cannot explain the external zones of constant composition observed along profiles on the majority of plagioclase self-contacts (Fig. 8).

Alternatively, diffusional exchange with the overlying main liquid may potentially give rise to buffering of plagioclase composition. In this case, sedimentation rate of crystals will be a key parameter, low rates favouring buffering of crystal composition, higher rates favouring the production of zoned crystals typical of orthocumulates (Morse 1986). Indeed, at first glance, the systematic decrease in the core to rim variability of plagioclase composition with increasing stratigraphic height in the lower zone (i.e., Fig. 6) may be interpreted in terms of a gradual decrease in sedimentation rate as crystallization of the main magma proceeds. However, diffusional exchange is most efficient at high temperature, making this process an unlikely candidate to explain the constant composition of the *external* part of plagioclase grains (Fig. 8). Indeed, our observations imply that the interstitial liquid composition was buffered at *lower* temperature, after a period of in-situ crystallization. The only other plausible mechanism for elimination of interstitial liquid is through convectional exchange, resulting from gravitational instability. On the

floor of a crystallizing magma chamber such convectional exchange will occur if the density of the more evolved interstitial liquid is less than that of the overlying more primitive liquid. Given that temperature alone will tend to stabilise the cooler interstitial liquid, an unstable configuration must be the result of the influence of liquid composition on density. For this reason, this process is commonly referred to as compositional convection, and it has been proposed as a potential mechanism for efficient adcumulus growth (e.g., Morse 1969, 1986; Tait et al. 1984; Tait and Jaupart 1996).

Although compositional convection alone cannot explain the characteristics of plagioclase from the lower zone of the Skaergaard, a period of in-situ crystallization followed by the onset of compositional convection can qualitatively account for our observations in this part of the intrusion. Such behaviour would require a transition from a trend of increasing liquid density during cooling (giving rise to in-situ crystallization), to one of decreasing liquid density (provoking convection). In other words, this would imply that liquids passed through a density maximum along the liquid line of descent. Given that the local liquid line of descent during interstitial crystallization should be similar at all levels of the intrusion, the density maximum should occur at approximately the same point along the differentiation trend, independently of stratigraphic height. This scenario therefore provides an elegant explanation for the observation that the inferred onset of liquid mobility systematically occurs when the local liquid was in equilibrium with a plagioclase of approximately *constant* composition (Fig. 6). Furthermore, consumption of post-cumulus liquid by convectional exchange can also explain the presence of buffered overgrowths on plagioclase rims (Fig. 8).

Before considering the implications of this scenario for the compositional evolution of the liquid, we note that compositional convection also requires that permeability is sufficiently high for exchange to occur, and that the time-scale of exchange (a function of density differences and liquid viscosity) is rapid relative to diffusive exchange and cooling. At the base of a basaltic magma chamber such as the Skaergaard, liquid viscosities are relatively low and porosities and permeabilities are initially high, in particular if an open touching framework of plagioclase exists (i.e., Philpotts et al. 1999; Jerram et al. 2003). Compositional convection can therefore be efficient in the LZ, although high local values of sedimentation rate may hinder the development of this process and lead to some dispersion in plagioclase rim composition. Furthermore, during the final stages of cooling a permeability threshold may be reached, leading to local patches of plagioclase of low X_{An}. The presence of evolved outliers (Figs. 2, 5), which decrease in abundance with increasing stratigraphic height in the LZ, and the fact that an incompatible element-rich component would appear to be present in the lower part of the LZ (Paster et al. 1974; Jang and Naslund 2001) are consistent with the existence of a population of evolved melt pockets trapped by a permeability threshold. At the top of the UZ the increasing abundance of albite-rich outliers (Fig. 2) may be explained in terms of increasing viscosity of the liquid due to temperature and/or compositional effects, which will drastically reduce the time-scale of convectional exchange.

One other point of interest is the observation that in rocks of the LZa the compositions of plagioclase rims in contact with minerals other than plagioclase and Fe–Ti oxides are statistically richer in anorthite component than plagioclase self-contacts (e.g., Figs. 6, 7). Furthermore, no plagioclase more evolved than An_{50} is in contact with minerals other than plagioclase (Fig. 6) implying that residual melt pockets trapped by permeability only occur between plagioclase grains (i.e., melt in contact with mafic minerals is completely eliminated by compositional convection). Both of these observations suggest that liquid–plagioclase contacts are energetically favourable compared to liquid–olivine or liquid–pyroxene contacts. Indeed, melt–solid dihedral angles are lower for melt–plagioclase–plagioclase contacts compared to melt–olivine–olivine or melt–pyroxene–pyroxene contacts (Holness 2006) providing independent evidence in favour of this hypothesis.

Returning to the question of the compositional evolution of the liquid, we have calculated the variation in density along the various liquid lines of descent proposed in the literature. At one extreme, the LLD characterised by increasing iron and decreasing silica proposed by McBirney and Naslund (1990) shows a continuous increase in density from the base to the top of the layered series (Fig. 9), behaviour which is incompatible with the observed variations of plagioclase composition presented here. Alternatively, the liquid lines of descent proposed by Tegner (1997) and Wager (1960) do pass through a density maximum, but at a stratigraphic level well above the base of the MZ (Fig. 9). In these cases too, the calculated evolution of liquid density is difficult to reconcile with our observations. On the other hand, liquid lines of descent characterised by silica enrichment associated with the appearance of cumulus magnetite (Hunter and Sparks 1987; Toplis and Carroll 1995; 1996) are calculated to experience a density maximum near the top of the lower zone (Fig. 9), in excellent first-order agreement with our observations. If the core-rim variations of plagioclase composition are indeed controlled by a density overturn in the liquid caused by saturation of Fe–Ti oxides then evidence for those oxides should be found in rocks of the lower zones a and b. Our own petrographic observations and those of Wager and Brown (1968; Table 5) show that oxide proportions are

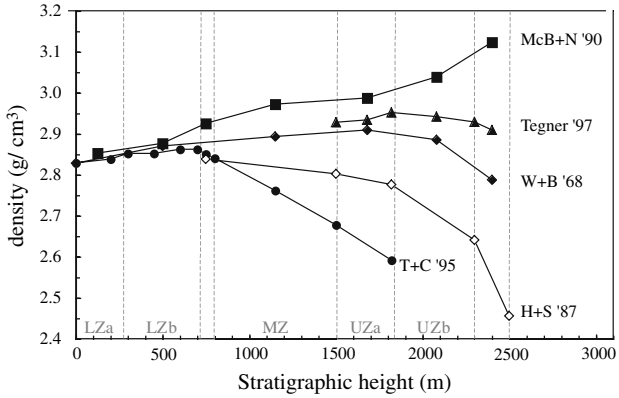

Fig. 9 Densities of liquids proposed for the Skaergaard Intrusion (calculated using Lange and Carmichael 1990, employing temperatures proposed by McBirney and Naslund 1990) plotted as a function of approximate stratigraphic height (using Wager and Brown 1968). *Solid squares* (McBirney and Naslund 1990) are liquids from McBirney and Naslund (1990); *solid triangles* are liquids from Tegner (1997); *solid diamonds* (Wager and Brown 1968) are liquids from Wager and Brown (1968); *open diamonds* (Hunter and Sparks 1987) are liquids calculated from a parental melt with 50 wt% SiO_2 by Hunter and Sparks (1987); *open circles* (Toplis and Carroll 1995) are experimental data of Toplis and Carroll (1995) for experiments along the FMQ buffer. These latter data have been placed using phase appearance and changes in X_{An} as a guide to equivalent stratigraphic height

typically 1–2 vol% in this part of the intrusion. Assuming that these rocks are composed of ~35% 'interstitial liquid' (Wager 1960), that ~50% of this liquid must crystallize to reach oxide saturation (using relative sub-zone sizes from Nielsen 2004), that the cotectic proportion of oxides is a generous 20% by mass once saturation is reached (Toplis and Carroll 1995), and that a mass to volume correction factor of 3/5 for the oxides is necessary, an oxide proportion of ~2 vol% is calculated, in good agreement with petrographic observation. However, in detail, it is of note that the density maximum of experimentally produced liquids (Toplis and Carroll 1995) occurs concurrently with the first appearance of magnetite, whereas the convergence of plagioclase core and rim compositions described here clearly occurs towards the top of the LZc rather than at its base (Fig. 6). One possibility for this offset is that a sufficient density *difference* must be built up to drive compositional convection, thus displacing the onset of liquid movement to stratigraphic levels slightly higher than the first appearance of cumulus magnetite. Alternatively, the base of the LZc may not represent saturation of the liquid in cumulus magnetite, a suggestion made by Jang et al. (2001) based upon the variation of vanadium in augite throughout the LS of the intrusion. In either case, a maximum in liquid density can be related to magnetite saturation, resulting in compositional convection and efficient adcumulus growth in the MZ.

Conclusions

Detailed study of plagioclase compositions of rocks throughout the layered series of the Skaergaard intrusion shows that although core compositions vary continuously from the base of the lower zone to the top of Upper Zone, rim compositions shows little variation throughout the lower portion of the intrusion, having a value of $An_{50 \pm 1}$ from the LZa to the lower MZ. Above the upper LZc where core and rim compositions converge, X_{An} of rim compositions decreases with height, generally overlapping the corresponding core compositions. Furthermore, compositional profiles across individual plagioclase grains in samples from the lower zone show that the majority of grains in contact with another plagioclase crystal show an external zone of variable width over which X_{An} has a constant value of ~50 ± 1. In this part of the intrusion the variations of plagioclase composition are consistent with a period of in-situ growth from an immobile intercumulus liquid, followed by a period during which the remaining liquid was replaced and buffered at constant composition. The simplest scenario capable of explaining all of the observed features is that during postcumulus crystallization in the lower zone, interstitial liquids reached a density maximum shortly after local saturation in magnetite, leading to compositional convection once an Fe–Ti oxide had appeared on the local liquidus. This scenario can explain the transition from orthocumulate textures in the LZa to adcumulate textures in the MZ. Although the data presented here cannot be used directly to identify the compositions of the Skaergaard liquids, the existence of a density maximum implied by our observations provides an important constraint which may be used to assess the validity of independently determined liquid lines of descent.

Acknowledgments We are particularly indebted to our friends and colleagues who generously donated rock samples, before our memorable visit to the intrusion in 2001. Those people include Graham Chinner (University of Cambridge), Alex McBirney (University of Oregon), Ian Parsons, Brian Upton and Peder Aspen (University of Edinburgh) and Kevin Walsh (University of Oxford Museum). Thanks also to S. Barda, F. Diot and A. Kohler of the Service Commun d'analyse of the Université Henri Poincaré in Nancy for help with the electron microprobe and SEM. S.A. Morse and an anonymous reviewer are thanked for their comments which were greatly appreciated. Financial support from the CNRS-INSU ("Intérieur de la Terre" and "Dyeti" programmes) is also acknowledged.

References

Andersen JCø, Rasmussen H, Nielsen TFD, Røngsbo JG (1998) The Triple Group and the Platinova gold and palladium reefs in the Skaergaard intrusion: stratigraphic and petrographic relations. Econ Geol 93:488–509

Brooks CK, Nielsen TFD (1990) The differentiation of the Skaergaard intrusion. A discussion of Hunter and Sparks (Contrib Mineral Petrol 95: 451–461). Contrib Mineral Petrol 104:244–247

Gibb FGF, Henderson CMB (1996) The Shiant Isles Main Sill: structure and mineral fractionation ranges. Mineral Mag 60:67–97

Grant NK, Chalokwu CI (1998) The cumulate paradigm affirmed. J Geol 106:641–644

Henderson P (1970) The significance of the mesostasis of basic layered igneous rocks. J Petrol 11:463–473

Henderson CMB, Gibb FGF (1983) Felsic mineral crystallization trends in differentiating alkaline basic magmas. Contrib Mineral Petrol 84:355–364

Holness MB (2006) Melt-solid dihedral angles of common minerals in natural rocks. J Petrol 47:791–800

Hoover JD (1989) Petrology of the Marginal Border Series of the Skaergaard intrusion. J Petrol 30:399–439

Hunter RH (1996) Texture development in cumulate rocks. In: Cawthorn RG (ed) Layered intrusions. Elsevier, Amsterdam, pp 77–101

Hunter RH, Sparks RSJ (1987) The differentiation of the Skaergaard intrusion. Contrib Mineral Petrol 95:451–461

Hunter RH, Sparks RSJ (1990) The differentiation of the Skaergaard intrusion. Reply to McBirney and Naslund. Contrib Mineral Petrol 104:248–254

Irvine TN, Andersen JCø, Brooks CK (1998) Included blocks (and blocks within blocks) in the Skaergaard intrusion: geologic relations and the origins of rhythmic modally graded layers. Geol Soc Am Bull 110:1398–1447

Jang YD, Naslund HR (2001) Major and trace element composition of Skaergaard plagioclase; geochemical evidence for changes in magma dynamics during the final stage of crystallization of the Skaergaard intrusion. Contrib Mineral Petrol 140:441–457

Jang YD, Naslund HR, McBirney AR (2001) The differentiation trend of the Skaergaard intrusion and the timing of magnetite crystallization: iron enrichment revisited. Earth Planet Sci Lett 189:189–196

Jerram DA, Cheadle MJ, Philpotts AR (2003) Quantifying the building blocks of igneous rocks: are clustered crystal frameworks the foundation? J Petrol 44:2033–2051

Lange RL, Carmichael ISE (1990) Thermodynamic properties of silicate liquids with emphasis on density, thermal expansion and compressibility. In: Nicholls J, Russell JK (eds) Modern methods of igneous petrology: understanding magmatic processes. Reviews in Mineralogy, vol 24, Chap 2, pp 25–64

Maaløe S (1976) Zoned plagioclase of the Skaergaard intrusion, East Greenland. J Petrol 17:398–419

McBirney AR (1989) The Skaergaard Layered Series: I. Structure and average compositions. J Petrol 30:363–397

McBirney AR (1996a) The Skaergaard intrusion. In: Cawthorn RG (ed) Layered intrusions. Elsevier, Amsterdam, pp 147–180

McBirney AR (1996b) Geological map of the Skaergaard intrusion, East Greenland, 1: 20,000. Department of Geology, University of Oregon, USA

McBirney AR, Hunter RH (1995) The cumulate paradigm reconsidered. J Geol 103:114–122

McBirney AR, Naslund HR (1990) The differentiation of the Skaergaard intrusion. A discussion of Hunter and Sparks (Contrib Mineral Petrol 95:451–461). Contrib Mineral Petrol 104:235–240

McBirney AR, Noyes RM (1979) Crystallization and layering of the Skaergaard intrusion. J Petrol 20:487–544

McBirney AR, Sonnenthal EL (1990) Metasomatic replacement in the Skaergaard intrusion, East Greenland: preliminary observations. Chem Geol 88:245–260

Meurer WP, Boudreau AE (1998) Compaction of igneous cumulates Part I: geochemical consequences for cumulates and liquid fractionation trends. J Geol 106:281–292

Meurer WP, Meurer MES (2006) Using apatite to dispel the "trapped liquid" concept and to understand the loss of interstitial liquid by compaction in mafic cumulates: an example from the Stillwater Complex, Montana. Contrib Mineral Petrol 151:187–201

Morse SA (1969) The Kiglapait layered intrusion, Labrador. Mem Geol Soc Am 112

Morse SA (1984) Cation diffusion in plagioclase feldspar. Science 225:504–505

Morse SA (1986) Convection in aid of adcumulus growth. J Petrol 27:1183–1214

Morse SA (1990) The differentiation of the Skaergaard intrusion. A discussion of Hunter and Sparks (Contrib Mineral Petrol 95:451–461). Contrib Mineral Petrol 104:240–244

Morse SA (1998) Is the cumulate paradigm at risk? An extended discussion of the cumulate paradigm reconsidered. J Geol 106:367–370

Naslund HR (1984) Petrology of the Upper Border Series of the Skaergaard intrusion. J Petrol 25:185–212

Nielsen TFD (2004) The shape and volume of the Skaergaard intrusion, East Greenland: imlpications for mass balance and bulk composition. J Petrol 45:507–530

Paster TP, Schauwecker DS, Haskin LA (1974) The behavior of some trace elements during solidification of the Skaergaard layered series. Geochim Cosmochim Acta 38:1459–1477

Philpotts AR, Brustman CM, Shi JY, Carlson WD, Denison C (1999) Plagioclase-chain networks in slowly cooled basaltic magma. Am Mineral 84:1819–1829

Shimizu N (1978) Analysis of the zoned plagioclase of different magmatic environments: a preliminary ion-microprobe study. Earth Planet Sci Lett 39:398–406

Smith JV, Brown WL (1988) Feldspar minerals. Springer, Berlin, p 828

Stewart BW, DePaolo DJ (1990) Isotopic studies of processes in mafic magma chambers: 2. The Skaergaard intrusion, East Greenland. Contrib Mineral Petrol 104:125–141

Tait SR, Jaupart C (1996) The production of chemically stratified and adcumulate plutonic igneous rocks. Miner Mag 60:99–114

Tait SR, Huppert HE, Sparks RSJ (1984) The role of compositional convection in the formation of adcumulate rocks. Lithos 17:139–146

Tegner C (1997) Iron in plagioclase as a monitor of the differentiation of the Skaergaard intrusion. Contrib Mineral Petrol 128:45–51

Toplis MJ, Carroll MR (1995) An experimental study of the influence of oxygen fugacity on Fe–Ti oxide stability, phase relations, and mineral-melt equilibria in ferro-basaltic systems. J Petrol 36:1137–1170

Toplis MJ, Carroll MR (1996) Differentiation of ferro-basaltic magmas under conditions open and closed to oxygen: implications for the Skaergaard Intrusion and other natural systems. J Petrol 37:837–858

Wager LR (1960) The major element variation of the layered series in the Skaergaard intrusion and a re-estimation of the average composition of the hidden layered series and of the successive residual magmas. J Petrol 1:364–398

Wager LR (1963) The mechanism of adcumulus growth in the layered series of the Skaergaard intrusion. Mineral Soc Am Spec Pap 1:1–9

Wager LR, Deer WA (1939) Geological investigations in East Greenland, Part III. The petrology of the Skaergaard intrusion, Kangerdlugssuaq, East Greenland. Meddr Grønland, vol 105, p 352

Wager LR, Brown GM (1968) Layered igneous rocks. Oliver and Boyd, Edinburgh, p 588

Wager LR, Brown GM, Wadsworth WJ (1960) Types of igneous cumulates. J Petrol 1:73–85